Use of generalized hyperspherical Sturmian functions for a three-body break-up model problem

2013 J. Phys. B: At. Mol. Opt. Phys. 46 015202

(http://iopscience.iop.org/0953-4075/46/1/015202)

J. Phys. B: At. Mol. Opt. Phys. **46** (2013) 015202 (11pp) doi:10.1088/0953-4075/46/1/015202

Use of generalized hyperspherical Sturmian functions for a three-body break-up model problem

D M Mitnik[1,3], **G Gasaneo**[2,3] **and L U Ancarani**[4]

[1] Instituto de Astronomía y Física del Espacio (IAFE), and FCEyN, Universidad de Buenos Aires, C.C. 67, Suc. 28, (C1428EGA) Buenos Aires, Argentina
[2] Departamento de Física, Universidad Nacional del Sur, 8000 Bahía Blanca, Buenos Aires, Argentina
[3] Consejo Nacional de Investigaciones Científicas y Técnicas, Argentina
[4] Laboratoire de Physique Moléculaire et des Collisions, UMR CNRS 7565, Université de Lorraine, 57078 Metz, France

E-mail: dmitnik@df.uba.ar

Received 28 September 2012, in final form 8 November 2012
Published 17 December 2012
Online at stacks.iop.org/JPhysB/46/015202

Abstract
A hyperspherical Sturmian approach recently developed for three-body break-up processes is tested through an analytically solvable *S*-wave model. The scattering process is represented by a non-homogeneous Schrödinger equation in which the driven term is given by a Coulomb-like interaction multiplied by the product of a continuum wavefunction and a bound state in the particles' coordinates. The model contains most of the difficulties encountered in a real three-body scattering problem, e.g., non-separability in the electrons' spherical coordinates and Coulombic asymptotic behaviour, and thus provides an interesting benchmark for numerical methods. Since the Sturmian basis functions are constructed so as to include the correct asymptotic behaviour, a very fast convergence of the scattering wavefunction is observed. Excellent agreement is found with the analytical results for the associated transition amplitude. This holds true down to very low energies, a domain which is usually challenging as it involves huge spatial extensions. Within our method, such calculations can be performed without increasing significantly the computational requirements.

(Some figures may appear in colour only in the online journal)

1. Introduction

The quantal description of three-body break-up processes is a notoriously difficult problem and, at the same time, of fundamental importance in atomic and molecular physics. Thanks to the fast evolution of computational capabilities, and the development of efficient numerical methods, huge progress has been made. *Ab initio* time-independent methods such as the convergent close coupling [1], the J-matrix [2] and the exterior complex scaling [3], have yielded many successful results, including the single ionization of hydrogen and the double photoionization of helium. These different methods managed—numerically—to describe accurately a double continuum of a three-body Coulomb system, i.e. two electrons escaping from a nucleus; an overall satisfactory agreement between them is observed. However, the application of the same methods to other processes (e.g. double ionization of helium [4]) or specific kinematic domains does not yield the same picture, probably due to convergence issues. Indeed, we should point out that these—now well established methods—generally require an enormous amount of computational resources. Thus, though fantastic progress has been made, three-body break-up problems still offer huge challenges to theoreticians. Another related issue is the fact that the above methods use spherical coordinates. One major obstacle when solving three-body break-up processes is imposition of proper asymptotic boundary conditions, for which hyperspherical coordinates are known to be better suited. Indeed, when

the three particles are far from each other, the three-body wavefunction asymptotically behaves as a distorted spherical wave which depends on all the coordinates (Peterkop's asymptotics) [5, 6]. Thus, hyperspherical coordinates are more adequate than, say, interparticle distances for which slow convergency rates are usually encountered to describe such an asymptotic behaviour [7]. It is thus important to continue to develop alternative and complementary methods that can deal with numerous physical problems and possibly with reasonable computational resources. This is also related to the idea of envisaging the next step: the four-body problem.

Over the last few years, a spectral method based on generalized Sturmian functions in spherical coordinates has been proposed to deal with scattering and structure problems. The efficiency of the method was illustrated in a number of applications involving two-electron systems (see [8–13] and references therein). For Coulomb scattering problems, in particular, one provides the Sturmian basis functions with adequate outgoing flux asymptotic conditions. In this way, the expansion on the basis is restricted to the region where the interaction between the particles takes place. As some of the relevant physical information is already built into the basis functions themselves, the expansions convergence rate is considerably increased when calculating the scattering wavefunctions and transition amplitudes. The method transforms the Schrödinger equation into an algebraic problem which can be solved with standard matrix techniques.

To solve general three-body systems, a method based on the use of generalized hyperspherical Sturmian functions (GHSF) has been recently developed and different strategies may be envisaged [14, 15]. In the numerical study presented in this paper, the scattered wavefunction is evaluated through an expansion in terms of GHSF constructed with a complete set of coupled hyperangular Jacobi polynomials and hyperradial Sturmian functions, the latter already accounting for the appropriate boundary conditions. With such a property, the hyperspherical Sturmian approach is expected to be very efficient. It is the aim of this paper to illustrate this.

In [16], we have presented an *S*-wave three-body break-up model with most of the difficulties of the real problem (Coulomb potential and non-separability). The model is physically meaningful, and presents the great advantage of having an analytical solution. It therefore provides a very useful, complete and solid test to validate numerical methods. Moreover, as the analytical solution is known, the model may be used to explore how the three-body asymptotic regimes are reached in different domains and different kinematics. This may help in identifying possible convergence difficulties of existing *ab initio* methods, in particular, at low energies for which large spatial domains are usually required. In this paper, the model is used to validate the hyperspherical Sturmian approach mentioned above, and to illustrate its numerical efficiency.

Model calculations can be found throughout the collision literature; benchmark studies are useful, in general, as they allow us to put on a strong footing different numerical methods which do not necessarily yield converging results when applied to complicated scattering processes which involve several ingredients. When the model is close to the description of a given process, it serves also to provide physical insight (see, for example, [17–22] for ionization processes). However, the models do not necessarily involve physical interactions (see, e.g. [23, 24]), and do not necessarily produce measurable quantities, but serve to illustrate the efficiency of a novel numerical method or to intervalidate two different methods.

The model proposed here consists in solving a driven Schrödinger equation for the scattering wavefunction. The driven term is the product of a Coulomb-like potential in the hyperradius ρ by a bound-free initial asymptotic state (it is built as the symmetrized, or not, product of a standing spherical wave and a bound state). The Coulomb-driven Schrödinger equation corresponding to this model presents the main difficulties encountered in the real three-body case and has the remarkable property of admitting a known analytical solution [16]. As far as we know, no other meaningful examples of the three-body scattering model—with analytical solution—has been provided in the literature.

The rest of this paper is arranged as follows. In section 2.1, we present a general scattering problem, which is simplified by using the model presented in section 2.2; the model problem is then presented in hyperspherical coordinates in section 2.3. In section 2.4, GHSF with outgoing wave asymptotic behaviour are defined, and the numerical implementation to solve the scattering problem is presented. Numerical and analytical results are compared and discussed in section 3. Asymptotic and energies considerations are treated in section 3.3. Finally, a summary and some perspectives are given in section 4.

Atomic units are used throughout.

2. Theory

2.1. General scattering problem

A general three-body scattering problem requires the solution of the three-body Schrödinger equation

$$[\mathbf{H} - E]\Phi(\mathbf{r}_1, \mathbf{r}_2) = [\mathbf{T}_1 + \mathbf{T}_2 + V_1 + V_2 + \mathbf{V}_{12} - E] \times \Phi(\mathbf{r}_1, \mathbf{r}_2) = 0 \quad (1)$$

where $\mathbf{T}_i$ (i=1,2) are the kinetic energy operators and V are the interparticle potentials. Without loss of generality, we may consider a three-body scattering process in which an incident electron collides with a one-electron atom of nuclear charge Z. As a first step, we will consider an *S*-wave model, in which all one-electron angular momenta are zero. The radial three-body Coulomb Schrödinger equation describing the dynamics of this particular problem is

$$\left[-\frac{1}{2}\frac{\partial^2}{\partial r_1^2} - \frac{1}{2}\frac{\partial^2}{\partial r_2^2} - \frac{Z}{r_1} - \frac{Z}{r_2} + \frac{1}{r_{12}} - E\right]\Psi(r_1, r_2) = 0, \quad (2)$$

where r_i represent the electron–nucleus coordinates, r_{12} is the inter-electronic distance, $\Psi(r_1, r_2) \equiv r_1 r_2 \Phi(r_1, r_2)$ is the reduced radial solution, the total energy E is assumed positive, and unit reduced masses are taken for simplicity.

It is quite common in scattering theory (e.g, [25, 26]) to separate the solution of the scattering problem into two terms, the first term is the scattering solution Ψ_{sc}, and the second, Ψ_0,

represents the solution of a simplified-potential equation. The Schrödinger equation

$$[H-E]\Psi(r_1,r_2) = [H-E]\Psi_{\rm sc}(r_1,r_2) + [H-E]\Psi_0(r_1,r_2) = 0, \quad (3)$$

is then converted into a non-homogeneous equation for $\Psi_{\rm sc}$

$$[H-E]\Psi_{\rm sc}(r_1,r_2) = -[H-E]\Psi_0(r_1,r_2). \quad (4)$$

Generally, Ψ_0 represents an asymptotically prepared initial state. We assume that the target electron (particle 1) is bound to the nucleus with a binding energy E_1, and assume an incident electron (particle 2) having an energy $E_2 = \frac{k_2^2}{2}$. From these, we have a natural bound-free state $\Psi_0(r_1,r_2)$ given by the product of a bound-state $\psi_1(r_1)$ and a continuum free-electron state $\psi_{k_2}(r_2)$, such that

$$\left[-\frac{1}{2}\frac{\partial^2}{\partial r_1^2} - \frac{Z}{r_1} - E_1\right]\psi_1(r_1) = 0 \quad (5)$$

and

$$\left[-\frac{1}{2}\frac{\partial^2}{\partial r_2^2} - \frac{k_2^2}{2}\right]\psi_{k_2}(r_2) = 0. \quad (6)$$

The non-homogeneous Schrödinger equation (4) becomes

$$\begin{aligned}[H-E]\Psi_{\rm sc}(r_1,r_2) &= -[V_2+V_{12}]\Psi_0(r_1,r_2)\\ &= \left[\frac{Z}{r_2} - \frac{1}{r_{12}}\right]\psi_1(r_1)\psi_{k_2}(r_2)\\ &\equiv -W(r_1,r_2)\Psi_0(r_1,r_2) \equiv \varphi(r_1,r_2),\end{aligned} \quad (7)$$

where the driving term φ is called the source term and $W(r_1,r_2)$ is the interaction not solved by the chosen initial state Ψ_0. Of course, there is no way to distinguish between the different electrons. Expression (7) is written in that way for a simple presentation, but in our model problem the driven term is further symmetrized.

2.2. Scattering model problem

The model problem proposed in our previous work [16] involves the replacement of the potential and the source by a model potential

$$V_1 + V_2 + V_{12} \to \frac{\mathcal{C}}{\rho} \quad (8)$$

and the driven term by a model source

$$\varphi(r_1,r_2) \to \rho^t {\rm e}^{-a\rho}\frac{1}{2}\left[\frac{\sin(r_1)}{r_1}\frac{\sinh(r_2)}{r_2} + \frac{\sin(r_2)}{r_2}\frac{\sinh(r_1)}{r_1}\right], \quad (9)$$

respectively, where the hyperradius $\rho \equiv \sqrt{r_1^2+r_2^2}$. As discussed in that work, our model has several useful features. Firstly, by choosing the parameter a such that $\mathcal{R}(a) > 1$ and $t \geqslant -1$, the driven term can be associated with the physical product of a bound-free state $\psi_1\psi_k$ multiplied by a Coulomb-like potential, which is the source term requested in the real problem (7). The potential election conforms also a very useful choice, since it has similarities with the Temkin–Poet potential (and hence, with the real scattering potential), but represents a different type of correlation between the particles. The model problem, thus, is not separable, presents a level of difficulties similar to any typical three-body scattering problem, and furnishes a new test for the different numerical methods. It has an additional remarkable feature: it allows an analytical solution. In the following sections, we will present a numerical method designed to solve this model problem, and will compare the results with the analytic solutions obtained in [16].

2.3. Scattering model problem in hyperspherical coordinates

The Hamiltonian for a system of three particles of masses m_1, m_2 and m_3 can be written in terms of any of three pairs of Jacobi or mass-scaled Jacobi coordinates [14, 15]. They can be expressed in terms of a hyperradius ρ and five hyperangular coordinates (denoted collectively by ω_5). Leaving aside the polar angles, we shall simply use $\rho = \sqrt{r_1^2+r_2^2}$ and the hyperangle $\alpha = \arctan(r_2/r_1)$.

In hyperspherical coordinates, equation (2) is written as

$$[H-E]\Psi(\rho,\omega_5) = [T+V(\rho,\omega_5)-E]\Psi(\rho,\omega_5) = 0, \quad (10)$$

where $V(\rho,\omega_5)$ describes the interaction potentials between the particles, and the kinetic energy operator takes the form

$$T = -\frac{1}{2\mu}\left[\frac{1}{\rho^5}\frac{\partial}{\partial\rho}\left(\rho^5\frac{\partial}{\partial\rho}\right) - \frac{\Lambda^2}{\rho^2}\right], \quad (11)$$

where Λ^2 is the grand orbital angular momentum operator and μ is the three-body reduced mass $\mu = \sqrt{m_1m_2m_3/(m_1+m_2+m_3)}$ [14, 15].

The driven Schrödinger equation in hyperspherical coordinates, analogous to equation (7), is

$$\begin{aligned}[T+V(\rho,\omega_5)-E]\Psi_{sc}(\rho,\omega_5) &= -W(\rho,\omega_5)\Psi_0(\rho,\omega_5)\\ &= \varphi(\rho,\omega_5).\end{aligned} \quad (12)$$

Equation (12) must be solved requiring regularity at the origin and imposing pure outgoing asymptotic behaviour to $\Psi_{sc}(\rho,\omega_5)$ for $\rho \to \infty$. The source (9) may be conveniently expanded [16] in a series of Jacobi polynomials [27]

$$\Omega_n(\alpha) = \mathcal{N}_n\, {}_2F_1(-n, n+2, \tfrac{3}{2}; \sin^2\alpha), \quad (13)$$

with $\mathcal{N}_n = 4(n+1)/\sqrt{\pi}$ (see also the definition (22) and related properties in section 2.4), in such a way that

$$\varphi(\rho,\alpha) = \sum_{n=0}^{\infty} f_n(\rho)\Omega_n(\alpha), \quad (14)$$

where

$$f_n(\rho) = b_n\, {\rm e}^{-a\rho}\rho^{2n+t} \quad (15)$$

and

$$b_n = \frac{1}{\mathcal{N}_n}\frac{1}{2^{2n}\left(\frac{3}{2}\right)_n n!}\frac{[(-1)^n+1]}{2}. \quad (16)$$

In this contribution, we will consider both symmetric and asymmetric sources. The term involving $(-1)^n$ (respectively 1) in (16) is associated with the first term (respectively second) of the driven term (9). In the symmetric case, the summation in expansion (14) is limited to even numbers n only. In figure 1, we plot $\varphi(\rho,\alpha)\rho^{5/2}$ as a function of the more familiar spherical variable r_1 and r_2, for $a = 2$ and $t = 0$ (the factor $\rho^{5/2}$,

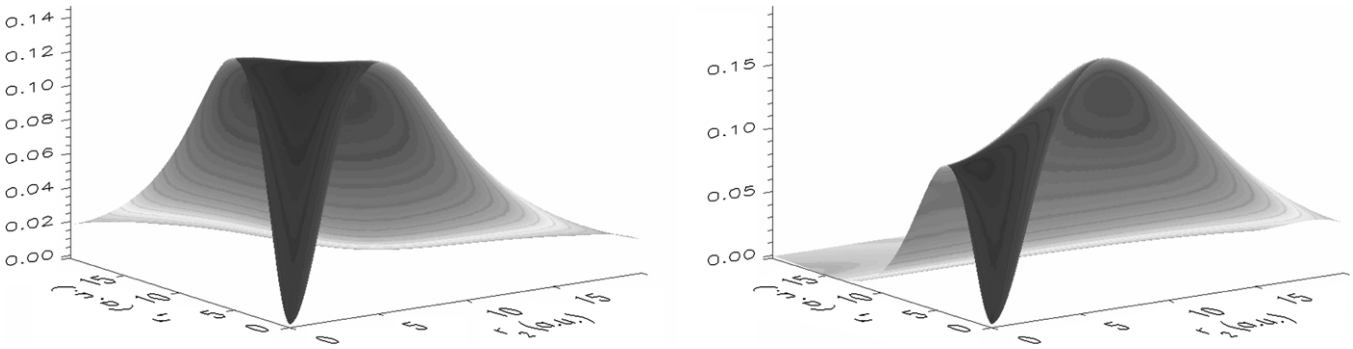

Figure 1. The source $\varphi(\rho,\alpha)\,\rho^{5/2}$, as it appears on the right-hand side of equation (19), is plotted as a function of the spherical coordinates r_1 and r_2 for the symmetric (left panel) and asymmetric (right panel) case. $\varphi(\rho,\alpha)$ is defined by equation (9), and here $t = 0$ and $a = 2$.

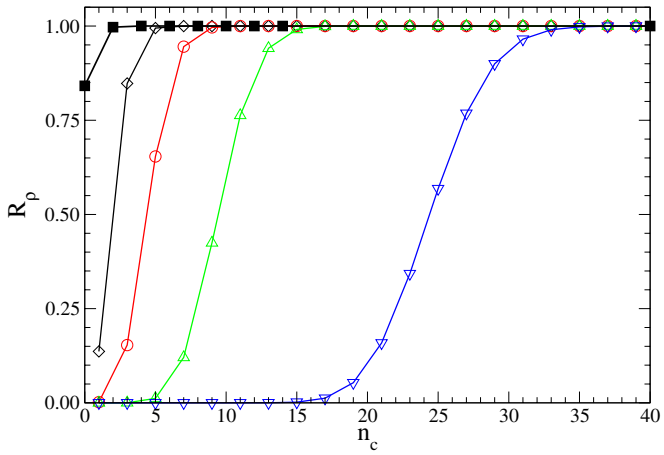

Figure 2. Convergence ratio $R_\rho(n_c)$ defined by equation (17) as a function of n_c, evaluated for $\alpha = 0$ and for different ρ values (unfilled symbols): diamonds ($\rho = 5$ au), circles ($\rho = 10$ au), triangles up ($\rho = 20$ au) and triangles down ($\rho = 50$ au). The filled squares represent the convergence ratio $R_\infty(n_c)$ defined by equation (36) for the numerical expansion of the transition amplitude.

that appears in the reduced form (19), is added for illustration purposes). In the left panel, the symmetric source (9) is shown, while the right panel illustrates the asymmetric source where only the first term in the squared bracket in (9) (or equivalently in (16)) is retained. The study of the latter will allow us, in section 3.2, to discuss symmetry and convergence issues. At large r_1 and r_2, the source behaves as the product of a Coulombic potential, multiplied by a decreasing exponential (representing a hydrogenic bound state) and a Bessel function (continuum state). Note that for r_i larger than say 5 au the source is already vanishing. The source function $\varphi(\rho,\alpha)$ is reproduced to an accuracy of 10^{-3} up to the hyperradius $\rho = 60$ through the expansion (14) with 45 terms. For larger hyperradii ρ, the number of terms needed in the expansion increases proportionally to ρ. The relationship between the number of terms needed for the expansion of the source at different hyperradius, and the hyperradius is illustrated in figure 2, where the following convergence ratio

$$R_\rho(n_c) \equiv \frac{\sum_{n=0}^{n_c} f_n(\rho)\Omega_n(\alpha)}{\varphi(\rho,\alpha)} \tag{17}$$

is shown for different hyperradii ρ. The calculations were performed for the hyperangle $\alpha = 0$, which is the case requiring the highest number of terms in the expansion.

In summary, the model driven Schrödinger equation we want to solve is

$$\left[-\frac{1}{2\mu}\left[\frac{1}{\rho^5}\frac{\partial}{\partial\rho}\left(\rho^5\frac{\partial}{\partial\rho}\right)-\frac{\Lambda^2}{\rho^2}\right]+\frac{\mathcal{C}}{\rho}-E\right]\Psi_{\rm sc}(\rho,\alpha) = \varphi(\rho,\alpha). \tag{18}$$

with the source (9) expanded as (14). Making the usual hyperspherical change of function $\Psi_{\rm sc}(\rho,\alpha) = \bar{\Psi}(\rho,\alpha)/\rho^{\frac{5}{2}}$, the equation to solve becomes

$$\left[-\frac{1}{2\mu}\frac{\partial^2}{\partial\rho^2}+\frac{\Lambda^2+15/4}{2\mu\rho^2}+\frac{\mathcal{C}}{\rho}-E\right]\bar{\Psi}(\rho,\alpha) = \rho^{5/2}\varphi(\rho,\alpha). \tag{19}$$

The analytical solution of the presented model was thoroughly studied in [16]. The general solution of the complete scattering problem is built as a linear combination of products of hyperradial functions with outgoing asymptotic behaviour times hyperangular $\Omega_n(\alpha)$ functions. The hyperradial functions are the sum of the general solution ($\chi_n(\rho)$) of the corresponding homogeneous equation and the particular solution ($R_n(\rho)$) of the non-homogeneous equation [28]. Thus, the total solution reads

$$\Psi^+(\rho,\alpha) = \frac{1}{\rho^{\frac{5}{2}}}\sum_n\left(\mathcal{A}_n\chi_n(\rho)+R_n(\rho)\right)\Omega_n(\alpha), \tag{20}$$

where the coefficients $\mathcal{A}_n$ are chosen in order to eliminate the incoming wave component of $R_n(\rho)$ [16, 28]. Asymptotically, we have the desired outgoing behaviour

$$\Psi^+(\rho,\alpha) \to f(\alpha)\frac{e^{i(K\rho-\eta\ln(2K\rho))}}{\rho^{\frac{5}{2}}}, \tag{21}$$

where K is the hyperspherical momentum related to the total energy $E = \frac{K^2}{2\mu}$ and $\eta = \frac{C\mu}{K}$ is the corresponding Sommerfeld parameter. This is the expected asymptotic behaviour for a Coulomb scattering problem [5]. This limit finally provides an analytical expression for the transition amplitude $f(\alpha)$.

2.4. Numerical implementation of the GSHF method

To numerically solve three-body break-up problems, a hyperspherical Sturmian approach has been recently

formulated [14, 15]. Different strategies can be followed to build GHSF. Here we will consider the following product of coupled functions. For the angular part, and for our S-wave problem, we solved the hyperangular eigenvalue equation

$$\Lambda^2\Omega_n(\alpha) = \left(q_n^2 - 4\right)\Omega_n(\alpha), \tag{22}$$

where Λ^2 is the S-wave simplified form of the grand angular operator. Analytically, the $\Omega_n(\alpha)$ are Jacobi polynomials, and $(q_n^2 - 4) = \lambda_n(\lambda_n + 4)$, with $\lambda_n = 2n$ $(n = 0, 1, ...)$ [27]. The eigenfunctions $\Omega_n(\alpha)$ form a complete set and satisfy the orthonormality relation

$$\int_0^{\pi/2} \Omega_n(\alpha)\Omega_m(\alpha)\sin^2\alpha\cos^2\alpha\,\mathrm{d}\alpha = \delta_{nm}. \tag{23}$$

Coupled to these angular polynomials, for a given n, we take as hyperradial basis functions, the Sturmian $S_{n,m}(\rho)$ satisfying the equation

$$\left[-\frac{1}{2\mu}\frac{\partial^2}{\partial\rho^2} + \frac{q_n^2 - 1/4}{2\mu\rho^2} + U(\rho) - E\right] S_{n,m}(\rho) = \beta_{n,m}\, V_g(\rho)\, S_{n,m}(\rho), \tag{24}$$

where $U(\rho)$ and $V_g(\rho)$ are, respectively, the auxiliary and the generating potentials; here E is externally fixed (as the energy of the system), while $\beta_{n,m}$ are the eigenvalues. All the basis functions $S_{n,m}(\rho)$ are regular on the whole domain. The potential $V_g(\rho)$ is assumed to be of short-range and we take $U(\rho)$ equal to the interaction potential, i.e. in our model problem $U(\rho) = \mathcal{C}/\rho$. With this choice, asymptotically, equation (24) reduces to a Coulomb homogeneous equation providing all basis GHSF, a unique—and appropriate—asymptotic behaviour, i.e. the one of the full solution sought after; for our problem, we choose outgoing behaviour

$$S^+_{n,m}(\rho) \to H^+_n(\eta, \rho), \tag{25}$$

where $H^+_n(\eta, \rho)$ is a linear combination of the regular and irregular Coulomb functions, and is defined and analysed for example in appendix A in [29]. We call ρ_0 the hyperradius value at which, numerically, this boundary condition is imposed. Since by construction, the asymptotic function only depends on the hyperangular quantum number n, and it is the same for all the hyperradial quantum numbers m, we can define a ρ-independent phase ϕ_n such that the asymptotic behaviour of the basis functions becomes

$$S^+_{n,m}(\rho) \to \mathrm{e}^{\mathrm{i}(K\rho - \eta\ln(2K\rho) + \phi_n)}. \tag{26}$$

For later discussions, we denominate ρ_σ the hyperradial distance beyond which the Coulomb function can be considered an outgoing function.

We thus expand the numerical solution of the scattering problem (18) with the above GHSF basis set

$$\Psi^{\mathrm{NUM}}(\rho, \alpha) = \frac{1}{\rho^{\frac{5}{2}}}\sum_m\sum_n a_{n,m}\; S^+_{n,m}(\rho)\;\Omega_n(\alpha). \tag{27}$$

Since both $\Psi^{\mathrm{NUM}}\rho^{5/2}$ and $S^+_{n,m}$ have the same asymptotic behaviour, the above expansion is restricted to the internal region where the interaction between the particles takes place. We first use the eigenvalue equation (22) for the angular part and then equation (24) for the radial part, so that equation (19) reduces to

$$\sum_m\sum_n a_{n,m}\;\beta_{n,m}\;\frac{V_g(\rho)}{\rho^{\frac{5}{2}}}\;S^+_{n,m}(\rho)\;\Omega_n(\alpha) = \varphi(\rho, \alpha). \tag{28}$$

Projecting over $S^+_{q,p}(\rho)\Omega_q(\alpha)/\rho^{\frac{5}{2}}$, integrating over ρ and α and using the orthonormality relation (23), the unknown coefficients $a_{n,m}$ are given by the following matrix equation:

$$\sum_m [\mathbf{SVS}]_{q,pm}\, a_{q,m} = I_{q,p}, \tag{29}$$

where the matrix elements $[\mathbf{SVS}]_{q,pm}$ are defined as

$$[\mathbf{SVS}]_{q,pm} = \int_0^\infty \beta_{q,m}\; S^+_{q,p}(\rho)\; V_g(\rho)\; S^+_{q,m}(\rho)\;\mathrm{d}\rho\,, \tag{30}$$

i.e. the overlap between the Sturmians under the generating potential. The right-hand side vector $I_{q,p}$ elements are defined by

$$I_{q,p} = \int_0^{\pi/2}\Omega_q(\alpha)\sin^2\alpha\cos^2\alpha\;\mathrm{d}\alpha\int_0^\infty S^+_{q,p}(\rho)\varphi(\rho,\alpha)\rho^{\frac{5}{2}}\mathrm{d}\rho. \tag{31}$$

Within the Sturmian approach, the Schrödinger equation (in our case the driven equation (19)) is transformed into an algebraic problem which can be easily solved using standard matrix techniques [14, 15, 12].

With the source (9) considered in our model, the angular integration coincides with the orthonormality property (23), and $I_{q,p}$ finally reduce to simple one-dimensional integrals:

$$I_{q,p} = b_q\int_0^\infty S^+_{q,p}(\rho)\,\mathrm{e}^{-a\rho}\rho^{2q+t}\rho^{\frac{5}{2}}\,\mathrm{d}\rho. \tag{32}$$

The transition amplitude can be easily extracted from $\Psi^{\mathrm{NUM}}(\rho, \alpha)$. Indeed, using the outgoing asymptotic behaviour (26), the wavefunction becomes

$$\Psi^{\mathrm{NUM}}(\rho, \alpha) \to \sum_m\sum_n a_{n,m}\frac{\mathrm{e}^{\mathrm{i}(K\rho - \eta\ln(2K\rho) + \phi_n)}}{\rho^{\frac{5}{2}}}\Omega_n(\alpha), \tag{33}$$

yielding, by comparison with (21),

$$f(\alpha) = \sum_n\left(\sum_m a_{n,m}\right)\mathrm{e}^{\mathrm{i}\phi_n}\Omega_n(\alpha). \tag{34}$$

3. Results

3.1. Numerical GHSF basis calculation

The calculations of the hyperangular basis polynomials $\Omega_n(\alpha)$ have been thoroughly studied in [14]. We solve numerically the hyperangular eigenvalue equation (22) by discretizing the functions in a uniform angular lattice. Within a finite-difference scheme and using a second-order approximation, a discretized version of this equation is obtained and solved using standard matrix diagonalization routines, such as those from a Lapack package [30]. As discussed there, we can obtain in our computation a very rapid convergence to the analytical

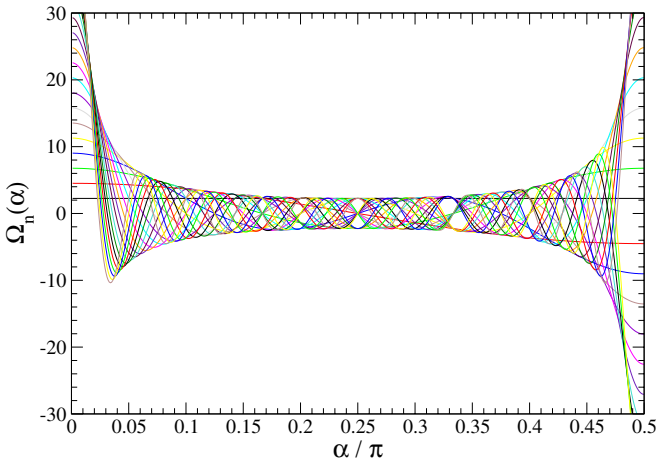

Figure 3. The first 20 eigenvectors of the hyperangular basis set $\Omega_n(\alpha)$.

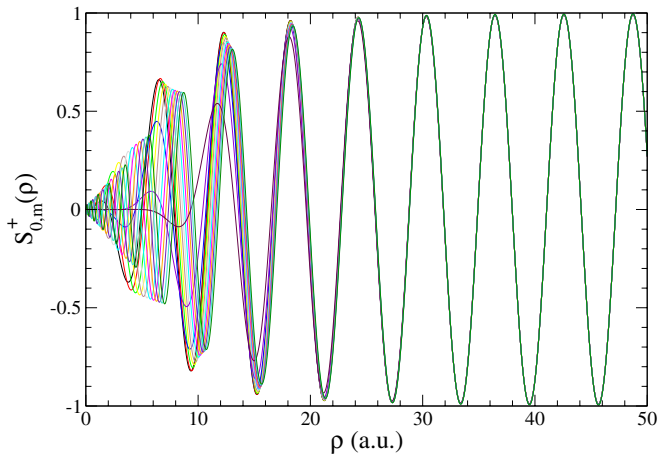

Figure 4. The first 15 generalized hyperspherical Sturmian basis set $S^{+}_{n,m}(\rho)$, for $n = 0$ and $E = 0.5$ au.

eigenvalues, by using a numerical grid having only a few number of points (less than 100). In figure 3, we show the first 20 eigenvectors of the angular basis set $\Omega_n(\alpha)$, obtained when solving equation (22) with a numerical grid having 500 points. Within this scale, the analytic (given by equation (13)) and numerical results are indistinguishable. The numerical eigenvalues are also very accurate; in the worst case (the largest eigenvalue), an error of less than 0.1% was obtained.

Different techniques can be implemented to numerically generate the GHSF, and we refer to [12] for details. The Sturmian equation (24) is numerically solved for different hyperangular n-quantum numbers, for the generalized potential $U(\rho) = \mathcal{C}/\rho$ with a model attractive charge $\mathcal{C} = -1$, assuming a reduced mass $\mu = 1$, and for an energy $E = 0.5$ au. The basis was calculated using a Yukawa generating potential

$$V_g(\rho) = -\frac{\exp(-\delta\rho)}{\rho} \tag{35}$$

where the range $\delta = 0.2$. We plot, in figure 4, the functions $S^{+}_{n,m}(\rho)$, corresponding to the first 15 hyperradial quantum numbers m, and for the hyperangular quantum number $n = 0$. The hyperradius ρ_0 at which the asymptotic boundary condition (25) is assumed determines univocally the eigenvalues and eigenvectors. Although for the particular choice of the parameter δ, the potential at $\rho = 30$ au is less than 10^{-4}, we impose the outgoing condition at a hyperradius $\rho_0 = 1500$ au, a choice that will be discussed in section 3.3. As shown in the figure, every function in the set achieves the asymptotic behaviour smoothly, and the set is dense for low hyperradial values. Therefore, any well-behaved function that vanishes for values $\rho < 15$ au can be perfectly expanded by this basis. For higher n values, the basis is dense for higher ρ values, allowing the expansion at a more extended range. The generating potential choice, and the adequate asymptotic behaviour, makes the basis very efficient as illustrated in the following section.

3.2. Numerical expansion in the GHSF basis

In this section, we present an illustration of the scattering solution and transition amplitudes, comparing the analytical results with the numerical GHSF expansion. We take hereafter the hyperspherical momentum of the system $K = 1$ au (i.e. the energy $E = 0.5$ au), the parameters of the source are taken to be $a = 2$ and $t = 0$ and the interaction charges as $\mathcal{C} = -1$ (a repulsive charge $\mathcal{C} = 1$ has also been tested, and provides similar results).

The GHSF used in our calculation were defined in such a way that all of them have the correct asymptotic behaviour of the problem fixed by the charge $\mathcal{C}$ and K, i.e. by the Sommerfeld parameter η. Thus, most of the Hamiltonian is diagonalized by the basis functions, and only the coupling produced by the driven term has to be dealt with. In that sense, the generating potential $V_g(\rho)$ has to be defined according to the source term. In our case, we need to expand the right-hand side of equation (18)—actually, it is the source $\varphi(\rho, \alpha)\rho^{5/2}$—which decreases very rapidly. As observed in figure 1, we can safely consider the source as zero, for hyperradial values of ρ larger than 20 au. This value limits the region defined as the driven region $\mathcal{R}_1$ in [16]. Again, the reason for choosing a much higher ρ_0 value for imposing the boundary condition in the basis generation procedure will be discussed later.

In figure 5, we plot the modulus of the numerical scattering solution $\Psi^{\mathrm{NUM}}(\rho, \alpha)\rho^{5/2}$ given by equation (27) (the modulus is shown as to avoid the oscillations which would crowd the figure). This function is the solution of the driven Schrödinger equation (18), for $E = 0.5$ au. To appreciate the symmetry related to that of the source (symmetric (left panel) and asymmetric (right panel) source), the solution is presented as a function of the more familiar spherical variable r_1 and r_2. The numerical results were obtained with 16 (only 8 for the symmetric case) hyperangular n- and 15 hyperradial m-terms. Overall excellent agreement (not shown as practically indistinguishable) is found with the analytical solution (20). A quantitative comparison is provided for the symmetric source, in figure 6, where the analytical solution is also shown (dotted line) as a function of ρ along the cut $\alpha = \pi/4$. We show the comparison at two regions, close to the origin (left) and at very large hyperradii (right). We also show separately the real (upper figures) and the imaginary (lower figures) part

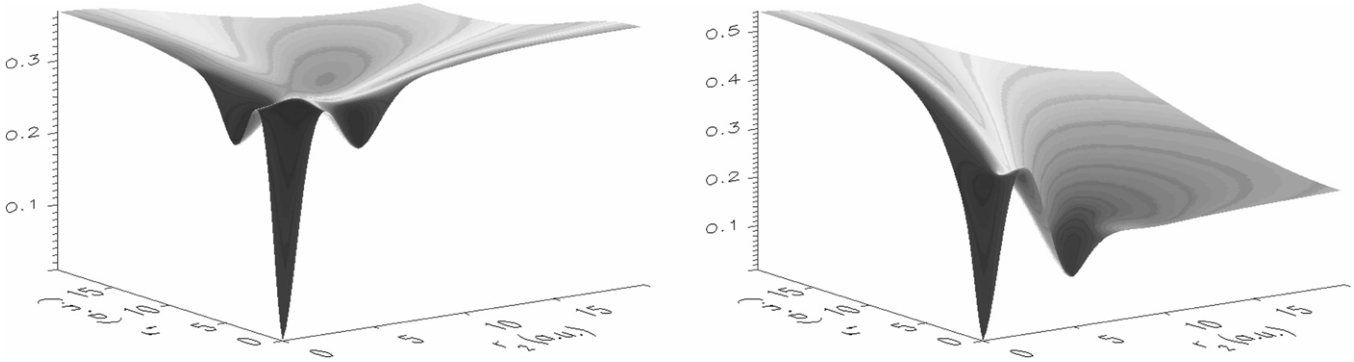

Figure 5. The modulus of the reduced numerical scattering solution $\Psi^{\mathrm{NUM}}(\rho,\alpha)\rho^{\frac{5}{2}}$ as given by equation (27) is plotted as a function of r_1 and r_2 for the symmetric (left panel) and asymmetric (right panel) source. The hyperspherical momentum $K = 1$ au, i.e. the energy $E = 0.5$ au.

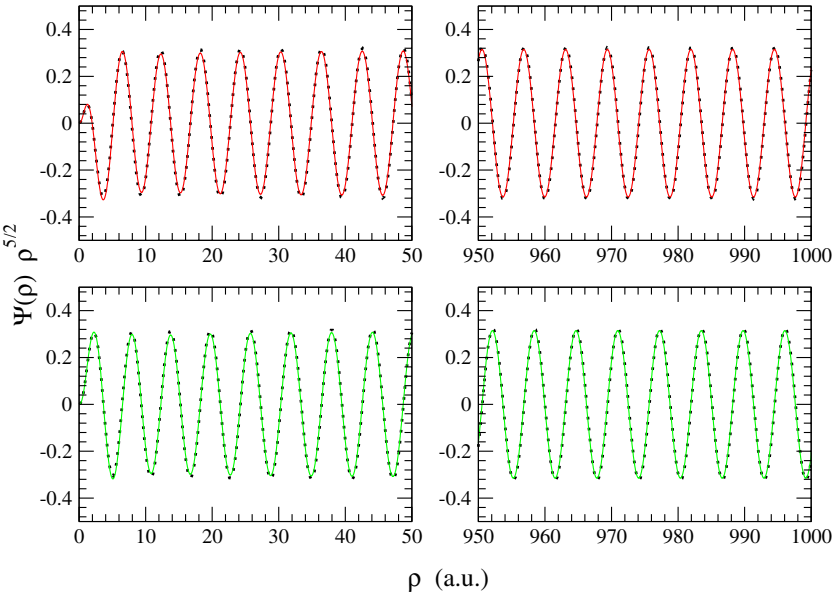

Figure 6. Upper figures: real part of the numerical (full line) scattering solution $\Psi^{\mathrm{NUM}}(\rho,\alpha)\rho^{5/2}$ given by equation (27) as a function of ρ along the cut $\alpha = \pi/4$, for $K = 1$ au; the dotted line is the real part of the analytical solution $\Psi^{+}(\rho,\alpha)\rho^{5/2}$ given by equation (20). Lower figures: the same functions, but the imaginary parts.

of the functions. In every case, a perfect agreement between the analytical and the numerical solutions, obtained with the GHSF method, is achieved.

Concerning the expansion in hyperangular quantum number terms, we have noted that an almost indistinguishable result can be obtained by using only a total of four terms in expansion (27). It is remarkable that although the source expansion (14) requires a large number of terms (specially for large ρ values), the expansion of the scattering solution (27) converges rapidly employing only a very few terms. This powerful characteristic is illustrated through figure 7, where the expansion coefficients $|a_{n,m}|$ are shown as a function of the hyperradial numbers m, for five hyperangular quantum numbers n.

We now turn to the transition amplitude. In figure 8, we compare the analytical result (20) obtained summing only the first eight terms, i.e. up to $n = 7$ (full line), with the one calculated numerically (dotted line) through expression (34). We show here, again, the cases with the symmetric (left panel) and asymmetric (right panel) sources. The symmetry with respect to $\alpha = \pi/4$ (i.e. $r_1 = r_2$) is clearly observed on the left panel. Coming back to figure 5, one can observe how, as r_1 and r_2 both increase (and thus ρ also), the value of the reduced function tends (see equations (33) and (34)) to the shape of the transition amplitude presented—in squared modulus—in figure 8. Finally, the very fast convergence of the numerical expansion (34) can be easily appreciated through the partial n summations (dashed lines); the exact result is reached to an accuracy of 10^{-4} with only three terms (summing the correspondent terms for $n = 0$, 2 and 4). In order to emphasize the extraordinary effectiveness of our numerical methods, we have also added, in figure 2, a curve (filled squares) representing the convergence of the transition amplitude

$$R_{\infty}(n_c) \equiv \frac{\sum_{n=0}^{n_c}(\sum_m a_{n,m}\Omega_n(\alpha))}{f(\alpha)} \tag{36}$$

as a function of the number of hyperangular terms needed in the numerical expansion (34). Since for the symmetric case only the even n-terms contribute to the sum, the number of terms included in each case is $n_c/2$. The results are given for the case $\alpha = 0$.

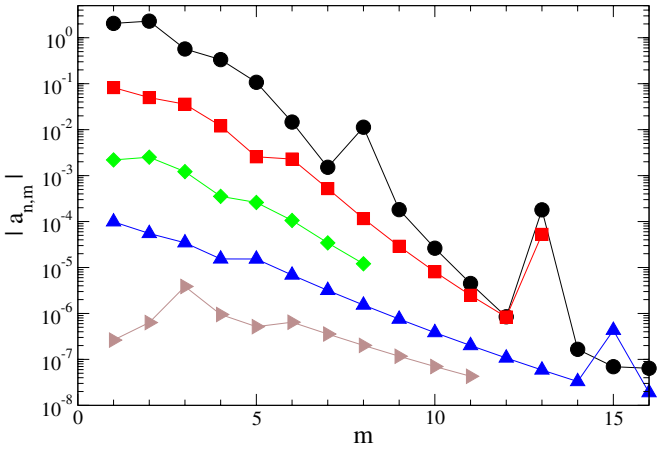

Figure 7. Modulus of the coefficients $|a_{n,m}|$ of equation (27) as a function of the hyperradial numbers m, for five hyperangular quantum numbers n: circles ($n = 0$), squares ($n = 2$), diamonds ($n = 4$), triangles up ($n = 6$) and triangles right ($n = 8$).

3.3. Asymptotic and energy considerations

Another important issue to investigate is the one related to the required distances to be reached in order to obtain convergent results, and, consequently, meaningful transition amplitudes. It was mentioned in section 3.1 that the asymptotic boundary condition (25) was imposed at a $\rho_0 > 1000$ au. Since the potential used in the Sturmian basis generation is negligible at a much lower distance (say $\rho \sim 20$ au), and then—as figure 4 shows—the basis functions already take their asymptotic behaviour, we need to clarify this choice. When we refer to the asymptotic condition, we must clearly distinguish between ρ values for the conditions prescribed for the basis generation, and for the scattering amplitude calculation.

Regarding the basis, the most important concern is to use a generating potential having a short range (in order to ensure the outgoing asymptotic condition), but sufficiently large in order to allow the correct representation of the solution expanded by this basis. A different argument is considered for the distances assigned to enforce the asymptotic condition when dealing with the proper scattering calculation. In this case, the outgoing asymptotic behaviour is an essential requirement to extract the scattering amplitude. When spanning the hyperradial domain, we first need to drive the expansion up to a region, named $\mathcal{R}_2$ in [16], where the required asymptotic behaviour begins. At this point, both the driven term and the generating potential can be safely considered as numerically zero, and the interaction appearing in the Hamiltonian dictates the dynamics and determines the solution to be the Coulomb function $H_n^+(\eta, \rho)$. For the parameters chosen in our generating potential, the lower limit of the region $\mathcal{R}_2$ can be assumed at a hyperradial distance of about $\rho_0 \sim 30$ au. Beyond this point, the solution is purely Coulombic. However, this range is still not appropriate for the scattering calculation because the Coulomb solution $H_n^+(\eta, \rho)$ does not possess—yet—a purely outgoing function. In order to ensure that the numerical expansion, equation (33), yields the amplitude (34), it is necessary to calculate the phase ϕ_n at a very large distance ρ_σ, located at the so-called region $\mathcal{R}_3$ (see [16]), where the Coulomb function becomes a truly outgoing wave. This region is well beyond the limit of region $\mathcal{R}_2$, and for the case studied here (the solution for an outgoing electron with an energy $E = 0.5$ au), one needs to go up to at least a distance of about $\rho_\sigma \sim 2000$ au. As a matter of fact, we calculate the phase ϕ_n through the numerical ratio of the Coulomb function $H_n^+(\eta, \rho_\sigma)$ to its asymptotic form

$$e^{i\phi_n} \equiv \frac{H_n^+(\eta, \rho_\sigma)}{e^{i(K\rho_\sigma - \eta \ln(2K\rho_\sigma))}}\,. \tag{37}$$

To recapitulate our numerical procedure, equation (29) is solved in the region $\mathcal{R}_2$, where the expansion coefficients $a_{n,m}$ of solution (27) are also determined. However, although the scattering wavefunction is obtained via this unique set of coefficients, the evaluation of the phase ϕ_n—and thus of the scattering amplitude $f(\alpha)$—varies with the considered hyperradius ρ_σ. This is illustrated through figure 9 where we plot the values of the scattering amplitudes at a hyperangle $\alpha = 0$, calculated with different choices of ρ_σ. As seen in the figure, although $\rho = 20$ au is a fair enough value to represent the expanded function, it is clearly not sufficient for the scattering amplitude calculation. We developed (see [12]) a very efficient computational code that allows us to generate the basis functions up to large distances, without any considerable

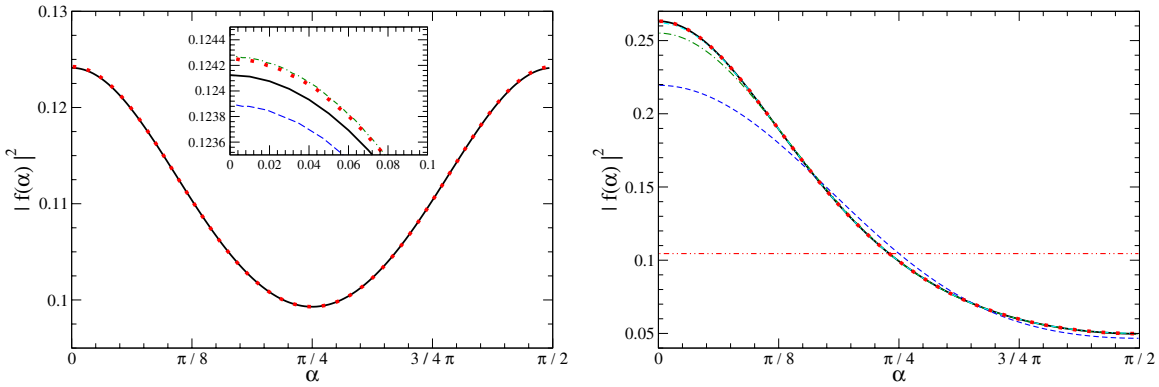

Figure 8. Analytical (full line) and numerical (dotted line) transition amplitude for $K = 1$ au, as a function of α for the symmetric (left panel) and asymmetric (right panel) source. Inset: partial summations (different hyperangular quantum numbers n in equation (34)) for the numerical transition amplitudes, with two terms (dashed line), three terms (dot–dashed line), and eight terms (dotted line). Right panel: partial summations with 1, 2, 3, 4 and 16 terms.

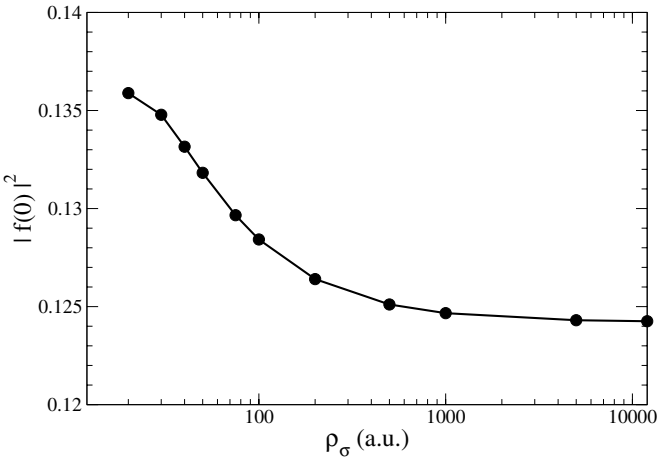

Figure 9. Transition amplitudes at $\alpha = 0$, calculated through equation (37) at different hyperradii ρ_σ.

computational effort. Therefore, although our choice of the parameter δ for the $V_g(\rho)$ potential (35) determines a short $\mathcal{R}_2$ range, we impose the boundary condition (25) at a much larger hyperradial value of $\rho_0 = 1500$ au. Once the expansion coefficients are determined there, we just need to calculate the sum of them (and the phase ϕ_n), at only one point ρ_σ, located at the outgoing asymptotic region $\mathcal{R}_3$. This hyperradius can be extremely large (20000 au), nevertheless, the computational requirements are immutable, since it is only one calculation. This feature distinguishes our method from other numerical techniques.

We can challenge our GHSF method, calculating the scattering amplitudes at other energies. It is well established that the convergence of the numerical methods is strongly energy dependent and becomes more difficult as the energy approaches the ionization threshold. An excellent example of this feature is found in the papers of Malegat and co-workers [31, 32], where the photoionization of He is studied under different conditions. In some of the calculations, they needed to propagate the evolution of the system up to a million atomic units. For this reason we have, therefore, repeated the calculations for the cases in which the outgoing electron has an energy of $E = 0.005$ au (hyperspherical momentum $K = 0.1$), and the resulting scattering amplitudes are displayed in figure 10 (left). The solid line represents the analytic results, and the dashed line is the GHSF numerical calculation. Note the excellent agreement between both calculations: for every angle, the error is less than 0.06%. In order to perform these calculations, a much more extended GHSF basis set has been used. By taking an exponential parameter $\delta = 0.005$ au in the generating potential (35), the basis functions achieve the Coulomb asymptotic behaviour at a hyperradius of about 1000 au. Although that is a fairly reasonably point to establish the region $\mathcal{R}_2$—and therefore, to perform there the coefficients calculation—we set up the asymptotic boundary condition at $\rho_0 = 15000$ au. On the right-hand side of figure 10, we show the convergence of the scattering amplitude (at $\alpha = 0$), as a function of ρ_σ. It is clear that calculating the amplitudes at hyperradii smaller than 500 au introduces a very large error in the final results.

The situation is even more challenging at lower energies. For the case in which the outgoing electron energy $E = 0.00125$ au ($K = 0.05$ au), we use the same GHSF basis as before, but now the scattering amplitude needs to be calculated at $\rho_\sigma = 150000$ au. In that case, an error larger than 10% is produced if the numerical grid size is smaller than 5000 au, and meaningless results are obtained when calculating the scattering amplitude with grids smaller than 1000 au. We found, as a rule of thumb, that for a hyperspherical momentum K, one should calculate the transition amplitudes at distances beyond $3000/K$. The transition amplitudes $|f(\alpha)|$ for $E = 0.00125$ are shown, as a function of the angle α, in figure 11 (left). In order to show the impressive agreement between the analytical and numerical HGSF results, both scattering wavefunctions along the cut $\alpha = \pi/4$ are shown in the right part of the figure, exhibiting an excellent agreement on the whole hyperradial range, for both the real (upper figures) and the imaginary (lower) parts of the solutions.

4. Summary and perspectives

In this paper, we have demonstrated the capability and efficiency of hyperspherical Sturmian functions to deal with three-body break-up problems. This was shown through the accurate reproduction of the analytical solution of a three-body

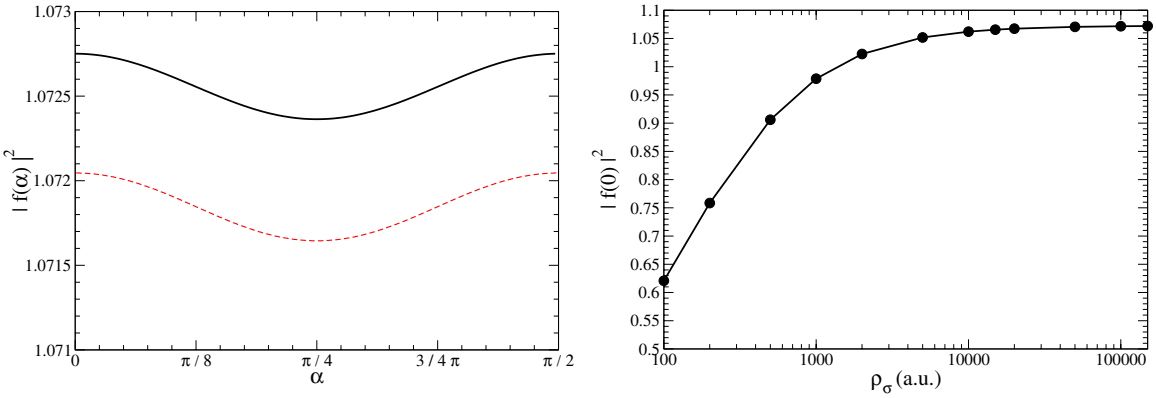

Figure 10. Left: analytical (full line) and numerical (dashed line) transition amplitude for $K = 0.1$ au ($E = 0.005$ au), as a function of the hyperangle α. Right: transition amplitudes at $\alpha = 0$, calculated at different hyperradii ρ_σ.

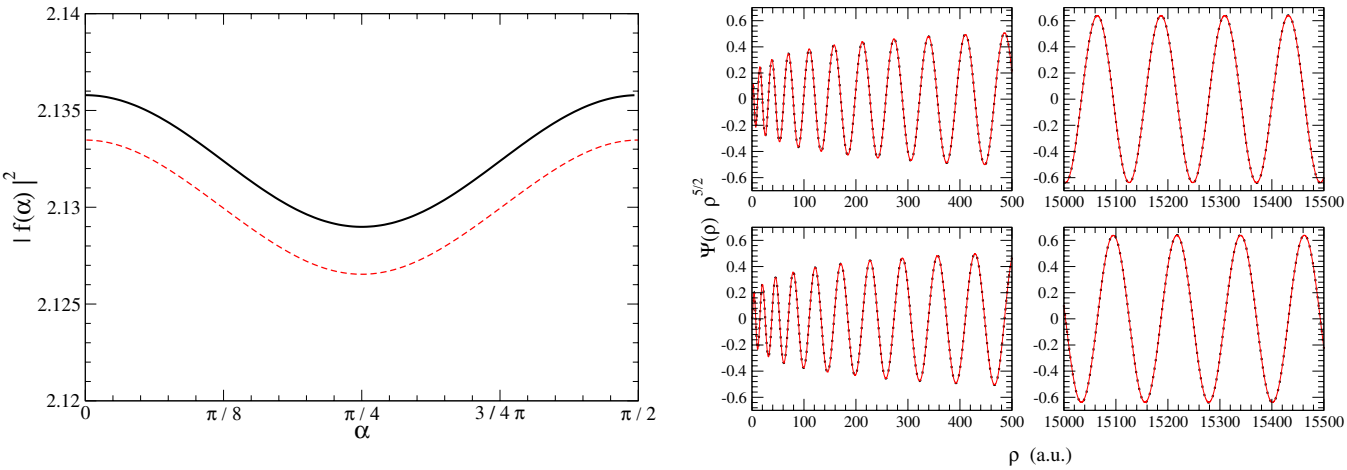

Figure 11. Left: analytical (full line) and numerical (dashed line) transition amplitude for $K = 0.05$ au ($E = 0.00125$ au), as a function of the hyperangle α. Right (upper figures): the real part of the numerical (full line) scattering solution $\Psi^{\mathrm{NUM}}(\rho, \alpha)\rho^{5/2}$ given by equation (27) along the cut $\alpha = \pi/4$; the dotted line is the real part of the analytical solution $\Psi^{+}(\rho, \alpha)\rho^{5/2}$ given by equation (20). Lower curves: same functions, the imaginary part.

S-wave ionization model. This model, which contains most of the difficulties of the real problem, consists in solving a driven Schrödinger equation with a Coulombic interaction in the hyperradius. The knowledge of a closed form of the solution and of the transition amplitude provides a solid benchmark to test numerical three-body methods; here, it is used to show that using optimal basis functions yield a very fast numerical convergence.

A hyperspherical Sturmian approach has been recently formulated to treat three-body break-up problems [14, 15]. Here, we used an expansion on a complete basis set of coupled hyperangular Jacobi polynomials and hyperradial Sturmian functions which account for appropriate asymptotic outgoing behaviour. All hyperradial basis elements not only diagonalize the kinetic energy and the interaction, but also possess the same appropriate asymptotic behaviour; they thus only need to expand the solution in the interaction region. These properties strongly accelerate the expansion convergence rate for the scattering wavefunction, and allow for a straightforward extraction of the transition amplitude. Excellent agreement with the analytical results is found with only very few expansion terms. The model driven Schrödinger equation is transformed into a straightforward algebraic problem which requires the evaluation of only Sturmian overlap matrix elements, and vector elements (involving the driven term) which, in our model, reduce to one-dimensional integrals.

The model problem proposed here allowed us to explore how the wavefunction takes different behaviours in different hyperradial domains, and how far one should go to extract the transition amplitude from the wavefunction itself. We found that the required hyperradial distances are very large, especially for low energies. With our GHSF method, we can reach the truly outgoing asymptotic region, where no other numerical method (besides the propagations performed by Malegat *et al* [31]) can handle the calculations.

The results presented in this contribution showed that the Sturmian hyperspherical approach is very efficient, with the hyperradial basis being ideally suited for the scattering problem under consideration. The next step is to explore the ability of the method to deal with more physical collision problems, with the final aim of considering the full three-body break-up situation with the full potential interaction. As an intermediate step, we plan to investigate first the corresponding Temkin–Poet model, in which the $1/r_{12}$ term is replaced by $1/r_{>}$ where $r_{>} = \max(r_1, r_2)$. In a longer term, it is then planned to apply the present hyperspherical Sturmian method (and a more elaborate version based on the formulation presented in [15]) to single and double ionization of atoms by electron or photon impact.

It is worth underlying once more that for three-body break-up processes, when all particles are far from each other, the Peterkop-type asymptotic behaviour

$$\Psi^{+}_{\mathrm{sc}}(\rho, \omega_5) \propto \rho^{-5/2}\, \mathrm{e}^{\mathrm{i}K\rho + \mathrm{i}\frac{\mathcal{C}(\omega_5)}{K}\ln(2K\rho)} \tag{38}$$

indicates that a hyperspherical approach should be more adequate than the use of interparticle (spherical) coordinates. The comparison of their efficiency, in particular with respect to asymptotic issues, is also part of our current investigations [7]. Formula (38) shows that, in the asymptotic region, the Coulomb interactions couple the angles with the hyperradius in a particular form, through the Coulomb logarithmic phase. All the angles, on the other hand, are coupled via the transition amplitude. These couplings arise from two sources: first, the non-separable character of the Coulomb interactions and, second, the coupling due to the driven term. By considering an appropriate initial state, the driven term turns out to be of short range. In that case, outside that range, the scattering wavefunction should satisfy a homogeneous Coulomb problem where, e.g, outgoing type behaviour should be imposed. Within our method, this could be easily achieved by using hyperradial functions having asymptotically fixed charge Coulomb behaviour. This can be further extended, as we can include parametrically the charge $\mathcal{C}(\omega_5)$ yielding the correct three-body behaviour to the generalized Sturmian functions (it should be underlined that such a method has nothing to do with effective charge approaches used to model double

continuum). We are considering using such an approach first for the Temkin–Poet model and then for the real physical problem. We expect to be able to evaluate the wavefunction up to very large distances being sure that we are having the correct wavefunction behaviour. This intrinsic property should provide optimal convergence.

Acknowledgments

One of the authors (GG) thanks the support by PGI (24/F049) of the Universidad Nacional del Sur, and DM the UBACyT 239 of Universidad de Buenos Aires. GG and DM also acknowledge the support of ANPCyT (PICT08/0934) (Argentina) and PIP 200901/552 CONICET (Argentina). This work has been developed within the activities planned in the French–Argentinian programme ECOS-Sud A10E01.

References

[1] Bray I and Stelbovics A T 1992 *Phys. Rev.* A **46** 6995
[2] Alhaidari A D, Heller E J, Yamani H A and Abdelmonem M S 2008 *The J-Matrix Method, Development and Applications* (Berlin: Springer)
[3] McCurdy C W, Baertschy M and Rescigno T N 2004 *J. Phys. B: At. Mol. Opt. Phys.* **37** R137
[4] Ancarani L U, Cappello C Dal and Gasaneo G 2010 *J. Phys.: Conf. Ser.* **212** 012025
[5] Rudge M R H 1968 *Rev. Mod. Phys.* **40** 564
[6] Peterkop R K 1977 *Theory of Ionization of Atoms by Electron Impact* (Boulder: Colorado Associated University Press)
[7] Randazzo J M *et al* 2012 in preparation
[8] Frapiccini A L, Randazzo J M, Gasaneo G and Colavecchia F D 2010 *J. Phys. B: At. Mol. Opt. Phys.* **43** 101001
[9] Frapiccini A L, Randazzo J M, Gasaneo G and Colavecchia F D 2010 *Int. J. Quantum Chem.* **110** 963
[10] Randazzo J M, Ancarani L U, Gasaneo G, Frapiccini A L and Colavecchia F D 2010 *Phys. Rev.* A **81** 042520
[11] Frapiccini A L, Randazzo J M, Gasaneo G and Colavecchia F D 2010 *Phys. Rev.* A **82** 042503
[12] Mitnik D M, Colavecchia F D, Gasaneo G and Randazzo J M 2011 *Comput. Phys. Commun.* **182** 1145
[13] Randazzo J M, Buezas F, Frapiccini A L, Colavecchia F D and Gasaneo G 2011 *Phys. Rev.* A **84** 052715
[14] Gasaneo G, Mitnik D M, Frapiccini A L, Colavecchia F D and Randazzo J M 2009 *J. Phys. Chem.* A **113** 14573
[15] Gasaneo G and Ancarani L U 2012 *J. Phys. A: Math. Theor.* **45** 045304
[16] Ancarani L U, Gasaneo G and Mitnik D M 2012 *Eur. Phys. J.* D **66** 270
[17] Temkin A 1962 *Phys. Rev.* **126** 130
[18] Poet R 1978 *J. Phys. B: At. Mol. Phys.* **11** 3081
[19] Pindzola M S, Mitnik D and Robicheaux F 1999 *Phys. Rev.* A **59** 4390
[20] Horner D A, McCurdy C W and Rescigno T N 2005 *Phys. Rev.* A **71** 012701
[21] Bartlett P L and Stelbovics A T 2010 *Phys. Rev.* A **81** 022715
[22] Bartlett P L and Stelbovics A T 2010 *Phys. Rev.* A **81** 022716
[23] Rescigno T N, Baertschy M, Byrum D and McCurdy C W 1997 *Phys. Rev.* A **55** 4253
[24] Rescigno T N and McCurdy C W 2000 *Phys. Rev.* A **62** 032706
[25] Newton R G 2002 *Scattering Theory of Waves and Particles* (New York: Dover)
[26] Joachain C J 1983 *Quantum Collision Theory* (Amsterdam: North-Holland)
[27] Abramowitz M and Stegun I A 1972 *Handbook of Mathematical Functions* (New York: Dover)
[28] Ancarani L U and Gasaneo G 2011 *J. At. Mol. Sci.* **2** 203
[29] Gasaneo G, Ancarani L U and Mitnik D M 2012 *Eur. Phys. J.* D **66** 91
[30] Lapack Linear Algebra Package www.netlib.org/lapack
[31] Malegat L, Selles P and Kazansky A K 2000 *Phys. Rev. Lett.* **85** 4450
[32] Malegat L, Bachau H, Hamido A and Piraux B 2010 *J. Phys. B: At. Mol. Opt. Phys.* **43** 245601